

Functional Finishing of Viscose Knitted Fabrics via Graphene Coating

Wen Wu^{1,2}, Huanxia Zhang^{1,2}, Hui Ma^{1,2}, Jianda Cao^{1,2}, Lianyi Jiang², Guanglin Chen²

¹Australia Institute for Advanced Materials and Manufacturing, Jiaxing University, Jiaxing, Zhejiang CHINA

²College of Material and Textile Engineering, Jiaxing University, Jiaxing, Zhejiang CHINA

Correspondence to:

Guanglin Chen email: chenguanglin644@163.com

ABSTRACT

Functional finishing of viscose knitted fabrics was realized through layer-by-layer assembly with graphene oxide and reduction treatment of hydrazine hydrate. Due to the introduction of graphene, viscose fabrics became conductive, and exhibited enhanced anti-ultraviolet properties and hydrophobicity. Scanning electron microscopy results demonstrated that graphene could form thin films on the surface of viscose fibers, and with an increase in dipping-drying cycles, partial peeling of the thin films was observed. Electrical resistivity tests indicated that the volume resistance could reach to 128 $\Omega \cdot \text{cm}$ and 96 $\Omega \cdot \text{cm}$ when the courses and wales of the viscose fabrics treated for thirty dipping-drying cycles. In addition, ultraviolet protection factor of the viscose fabrics was 100+ and the water contact angle of the viscose fabrics treated for twelve cycles was 125° compared with 18° for the original fabrics. These multifunctional fabrics have potential applications in conductive devices, water treatment systems and smart textiles.

Keywords: Viscose knitted fabrics; Graphene; Conductive properties; Anti-ultraviolet; Hydrophobic property

INTRODUCTION

Natural fiber composites and their applications areas have become of interest due to the high presence of polar groups, flexibility and low cost. Various types of functional materials, such as synthetic polymers, cyclodextrins, silver particles, titanium dioxide, silica, aluminum oxide, copper particles, and graphene can endow natural fibers or fabrics with water repellency, antimicrobial properties, self-cleaning tendencies, flame retardancy, conductivity and electromagnetic and ultraviolet (UV) shielding properties [1-9].

Graphene is conductive due to the restored sp² bond networks. As a result, functional composite materials can be produced through dipping (brushing) and drying of fabrics into graphene solutions or solution-spinning of regenerated cellulose and graphene, respectively [10, 11].

The dipping and drying process has been commonly employed to coat the fibers or fabrics with graphene layers. Flexible conductive devices based on reduced graphene oxide and cotton fabrics have been fabricated using this method by other researchers [12-15]. To further improve the conductivity of fabrics, poly (3,4-ethylenedioxythio-phenyl): poly(styrene sulfonate) or polyaniline was introduced during the coating process of graphene [16, 17]. Besides the dipping-drying method, some reports have demonstrated that the solution-spinning of regenerated cellulose and graphene could significantly improve mechanical and thermal properties of regenerated cellulose fibers [18].

Viscose, which is regenerated cellulose, has few crystalline regions and a large amount of polar groups, resulting in increased flexibility and reactivity. Herein, a method is proposed to fabricate functional viscose fabrics with improved properties by using layer-by-layer assembly of graphene oxide (GO) on viscose fabrics and reducing treatment of hydrazine hydrate. The structure change of GO and reduced graphene oxide (RGO), morphology of control and functionalized viscose fabrics were characterized by Fourier transform infrared spectroscopy (FT-IR), scanning electron microscopy (SEM) and X-ray diffraction (XRD). The electrical conductivity, anti-UV, hydrophobic properties and water laundering durability of different fabrics were also measured.

EXPERIMENTAL

Materials

A modified Hummer's method was utilized to fabricate GO from flake graphene (Provided from Sinopharm Chemical Reagent Co., Ltd) [19]. First, flake graphene was added into a mixture of H₂SO₄, sodium nitrate and KMnO₄. After agitation for 1 h at 0°C, distilled water and H₂O₂ were added to the mixture and sequentially stirred for 15 min. The mixture was centrifuged and the residues were washed with distilled water until a pH of 7 was achieved, and GO was collected.

Commercial viscose knitted fabrics (75 loops /5 cm and 109 loops /5 cm at course and wale respectively, 198 g/m²) were provided by the Suzhou Shuishan Industrial Co., Ltd. and cleaned with sodium hydrate solutions before use. Sulfuric acid, hydrogen peroxide, hydrazine hydrate, sodium nitrate and potassium permanganate were supplied by Sinopharm Chemical Reagent Co., Ltd.

Preparation of RGO-Viscose

Functionalized viscose fabrics were obtained using multi-cycle dipping-drying treatments with GO dispersions on the viscose fabrics (GO- Viscose) and a reducing treatment of GO-Viscose with hydrazine hydrate. The viscose fabrics were dipped into the 0.73g/L GO dispersion for 30 min and then dried at 50°C for 12 h. This process was repeated for as many cycles as required coat the GO layers onto viscose fibers. In the reducing process, GO-Viscose (5g) was immersed in N₂H₄·H₂O solutions (250 mL, 3%) and kept at 95°C for 3 h. The resulting fabrics were washed with distilled water and dried at 50°C and different RGO-Viscose fabrics were collected. Based on the number of repeated dipping-drying cycles required, the samples were defined as 1, 3, 5, 7, 9, 12, 15, 30 or 50-RGO-Viscose, respectively.

Characterization

The surface chemical structure of GO and RGO was characterized by FT-IR using a Nicolet 470 FT-IR spectrometer (Thermo Nicolet Corporation, USA) from 4000 to 500 cm⁻¹. A HITACHI S-4800 SEM was used to observe the morphology of the samples using an acceleration voltage of 1 kV. Before observing, samples were coated with Au in an E1010 sputter coater (HITACHI, Japan).

The structure of RGO-Viscose was characterized with a Rigaku Dmax 2500 PC diffractometer (Tokyo, Japan) operating at 40 kV ($\lambda=1.5418\text{\AA}$). The scanning range varied from 4° to 35°.

International Electro Technical Commission Procedure 93-1980 was used to study the electrical conductivity of original viscose and RGO- Viscose fabrics, and the value of volume resistance was calculated by the equation:

$$\rho v = R \cdot S/L \quad (1)$$

Where R is the electrical resistivity of fabrics (Ω); L is the distance between two electrodes (cm); S is the cross-sectional area of fabrics (cm²).

In order to evaluate the anti-UV properties of original and functionalized viscose fabrics, the average values of the ultraviolet protection factor (UPF) and the transmittance of UVA %, UVB % of samples were obtained via an YG (B) 912E UV spectrophotometer (Darong textile instrument, Zhejiang, China). According to the standard AS/NZS 4399: 1996, cellulose with a UPF ≥ 40 is considered to possess excellent protection against UV radiation. A video contact angle instrument (JC2000C1, Shanghai Zhongchen Digital Technic Apparatus Co., Ltd, Shanghai, China) was used to characterize the hydrophobic properties of samples and contact angles were also measured. Five measurements of different fabrics at 3s were carried out. Before testing, all samples were conditioned at standard atmospheric conditions for 48 h. The water laundering durability test of the RGO-Viscose was carried out according to AATCC Test Method 61-2006 using a washing laundering machine (SW-12J, Wenzhou Darong Co., Ltd., Zhejiang, China).

RESULTS AND DISCUSSION

Structure Change of GO and RGO

Figure 1 shows the FT-IR spectra of GO, RGO and various viscose fabrics. The GO layers presented different bands arising from oxidized groups. The peaks at 1390 cm⁻¹ and 1118 cm⁻¹ were attributed to the -OH deformation vibrations and C-OH stretching vibrations [20, 21]. After reduction treatment, the decreased peak intensities indicated that the oxidized groups on GO layers were partially removed.

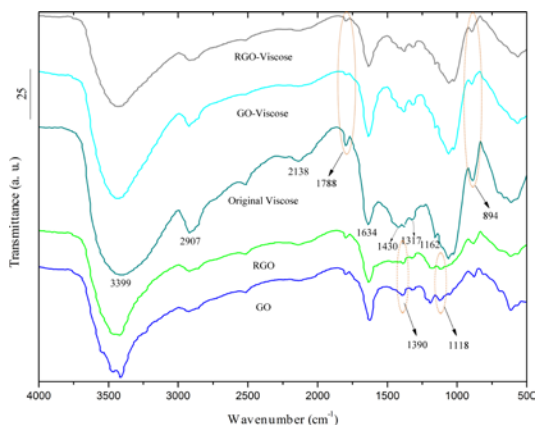


FIGURE 1. FTIR spectra of GO, RGO, original viscose, GO-Viscose and RGO-Viscose.

For the original viscose fabrics, the peaks at 3399 cm^{-1} , 2907 cm^{-1} , 1634 cm^{-1} , 1430 cm^{-1} and 1317 cm^{-1} correspond to the -OH stretching vibrations, -CH-stretching vibrations, -OH bending vibrations, -CH₂-stretching vibrations and -CH- bending vibrations respectively. Similar results were reported by M. S. Khalilabad and M. E. Yazdanshenas [14]. Peaks at 1788 cm^{-1} and 894 cm^{-1} in the spectra of GO-Viscose and RGO-Viscose are attributed to the -C=O and -C-C- stretching vibrations respectively [20, 22]. Peak intensities have decreased, indicating the formation of RGO films on the surfaces of the fibers.

Morphology of RGO-Viscose

Figure 2 shows the SEM images of original and functionalized viscose fibers. The surface of the original viscose fibers was grooved. After one cycle of RGO coating, the surface of 1-RGO-Viscose exhibited some corrugations and the RGO sheets were wrinkled (Figure 2B). When more RGO sheets were deposited, RGO films were observed, although the continuity of films was poor (Figure 2C). With further increases in coating cycles, especially for 30-RGO-Viscose and 50-RGO-Viscose (Figure 2E and 2F), the surface of viscose fibers was completely coated by continuous RGO films with the multilayer morphology, and the ridges and groves of the viscose fibers were no longer visible. However, the coating of high concentration of RGO sheets resulting from increasing dipping-drying cycles could lead to the formation of RGO clumps, and partial exfoliation of RGO films could be observed as shown in Figure 2E and 2F. The results were supported by FT-IR analysis, which revealed decreases in intensities of the -C=O and -C-C- stretching vibrations.

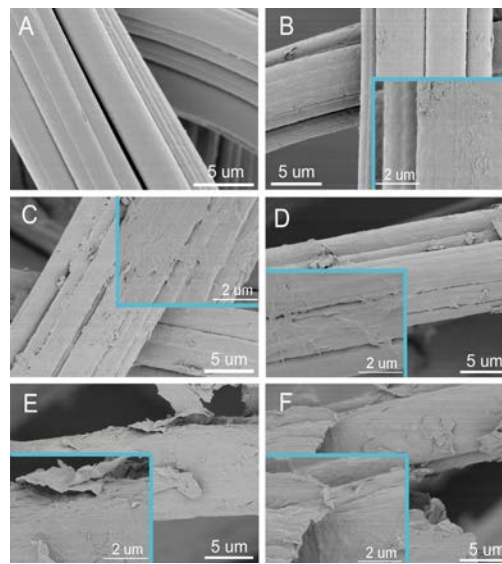


FIGURE 2. SEM images of original fibers (A), 1-RGO-Viscose (B), 5-RGO-Viscose (C), 12-RGO-Viscose (D), 30-RGO-Viscose (E) and 50-RGO-Viscose (F).

Structure of RGO-Viscose

Figure 3 shows the XRD spectra of original viscose fabrics and various RGO-Viscose fabrics. It can be observed that the XRD spectra of the original viscose fabrics exhibited a broad peak at 2θ of 22.5° , which was assigned to cellulose II [23]. The XRD spectra of RGO-Viscose fabrics showed similar diffraction peaks to those of original viscose fabrics, indicating that the coating of RGO films on fabrics did not change the nano-structure of the viscose fabrics.

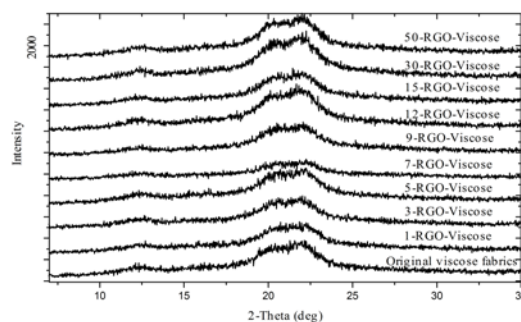


FIGURE 3. XRD spectra of different RGO-Viscose fabrics.

Electrical Conductivity of RGO-Viscose

Figure 4 shows the electrical resistivity of different RGO-Viscose fabrics at the course and wale. For 1-RGO-Viscose, the value of volume resistance at the

course and wale was $2.47 \times 10^4 \Omega \cdot \text{cm}$ and $1.97 \times 10^4 \Omega \cdot \text{cm}$ respectively, while the original viscose fabrics were hardly conductive- the value of volume resistance was too large to record. The reason that the volume resistance at the course was higher than that at the wale was due to loop formation resulting from knitting in the weft direction and the formation of sinker-loops in the warp direction. With increasing dipping-drying cycles, the volume resistance sharply decreased, especially for 30-RGO-Viscose- the values of volume resistance at the course and wale were $128 \Omega \cdot \text{cm}$ and $96 \Omega \cdot \text{cm}$, respectively.

Therefore, it can be concluded that increasing dipping-drying cycles promote electrical conductivity of whole fabrics and decrease the heterogeneity of electrical properties between the course and wale. These results are similar to those reported by some researchers [14, 16].

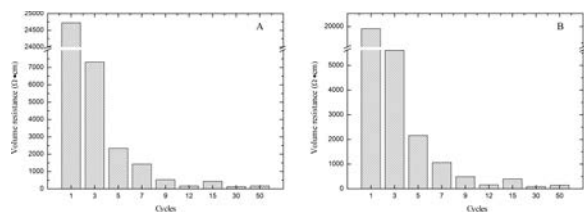


FIGURE 4. Electrical resistivity of different RGO- Viscose fabrics at course (A) and wale (B).

Anti-UV Properties of RGO-Viscose

Figure 5 shows the values of UVA % and UVB % of different RGO-Viscose fabrics. In this work, the UPF value of the original viscose fabrics was 1 and the value of UVA and UVB were 99.95 % and 99.32 % respectively. When the RGO layers were introduced, all the RGO-Viscose fabrics had the UPF values of 100+ and exhibited the excellent UV protection. In addition, UVA and UVB values of 1-RGO-Viscose showed sharp decreases- from 99.95% to 0.29 % and from 99.32 % to 0.20 %, respectively. With an increase in dipping-drying cycles, the concentrations of RGO layers increased, resulting in further decreases in UVA and UVB values. The minimum value (0.01%) of UVA and UVB were observed for RGO-Viscose fabrics after fifty coating cycles. The results demonstrated that RGO layers, which are two-dimensional crystalline sheets with carbon atoms densely packed in a sp^2 -bonded honeycomb lattice [24], could block UV rays and provide excellent UV protection to the fabrics when stacked through layer-by-layer assembly on the surface of fibers.

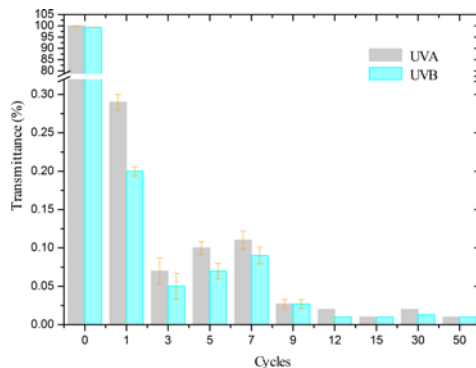


FIGURE 5 The UVA and UVB transmittance of different RGO-Viscose fabrics.

Hydrophobic properties of RGO-c-VF

Figure 6 shows the results of contact angle measurements of the original and different RGO-Viscose samples. Original viscose fabrics were hydrophilic and the water contact angle was 18° . Due to the introduction of RGO by one dipping-drying cycle, a substantial increase in water contact angle (from 18° to 119°) was observed. The RGO- Viscose fabrics loaded with more RGO layers showed further slight increases. The value of water contact angle of 12-RGO- Viscose was 125° . For knitted viscose fabrics, the results indicate that the introduction of low concentrations of RGO layers could endow the fabrics with hydrophobicity. Some researches had proved that graphene layers their own exhibited hydrophobic functionalities, which were related to the layer size and polar groups ($-\text{COOH}$, $-\text{OH}$, etc.) on the layers. After the reduction treatment of viscose fabrics with GO coatings, most polar groups were removed and the ratio of $\text{C}=\text{C}$ bonds increased, resulting in increasing hydrophobicity [25].

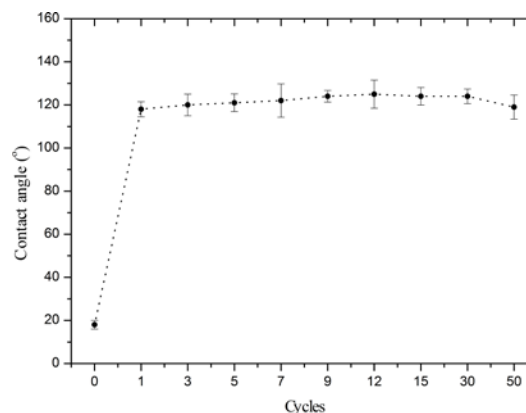


FIGURE 6. The water contact angles of original viscose and different RGO-Viscose fabrics.

Hydrophobic Properties of RGO-c-VF

Figure 7 shows the volume resistance of 12-RGO-Viscose with increasing water laundering times. As shown in Figure 7, the value of volume resistance was 128 $\Omega\cdot\text{cm}$ before the water laundering test. After eight times water laundering, the value of volume resistance increased from 128 $\Omega\cdot\text{cm}$ to 162 $\Omega\cdot\text{cm}$. With further increase in water laundering times, the value increased sharply and reached 210 $\Omega\cdot\text{cm}$. Thus, the results indicate that the RGO-Viscose exhibited good water laundering durability.

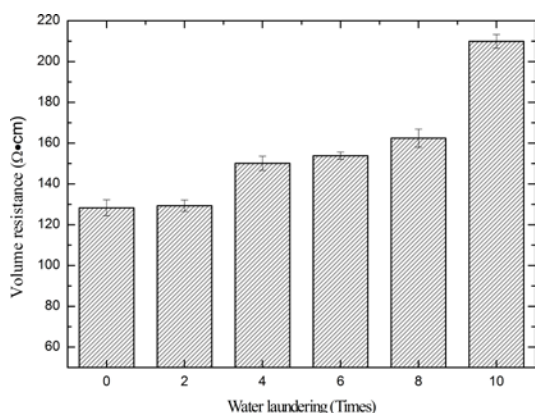


FIGURE 7. The change of volume resistance with the increase of water laundering times.

The fabrication of functional fabrics (conductivity, hydrophobic, UV-blocking, and so on) through the coating of RGO onto the fabrics has also been achieved by some other researchers [15, 25]. Tian et al. found that cotton fabrics could exhibit electrical resistivity of 2.29 $\Omega\cdot\text{m}$ and robust ultraviolet protective properties (a maximum UPF value of 312) after the doping of graphene and poly(3,4- ethylene dioxythiophene): poly(styrene sulfonate) and chitosan by layer-by-layer electrostatic self-assembly [16]. Such graphene-coated conductive cotton fabrics could exhibit less short-circuits current than the traditional Pt electrode and have potential applications as flexible energy storage devices [14].

CONCLUSION

In this work, a graphene oxide layer, which was a two-dimensional crystalline sheet with carbon atoms densely packed in a sp^2 -bonded honeycomb lattice, was coated onto the surface of viscose fibers using a multi-dipping-drying process. The results demonstrated that RGO layers were intermittently

absorbed on the surface of fibers at low concentrations, and with increasing concentrations of RGO layers, complete RGO films were formed. RGO-Viscose exhibited improved conductivity (128 $\Omega\cdot\text{cm}$ of the course and 96 $\Omega\cdot\text{cm}$ of the wale), anti-UV (0.01% of UVA and UVB transmittance) and hydrophobic properties (125° water contact angles) compared with the original viscose fabrics (very low conductivity, 99.95 % of UVA and 99.32 % of UVB transmittance, UPF of 1 and 18° water contact angles). This approach offers a practical method to significantly improve the electrical conductivity, anti-UV and hydrophobic properties of viscose fabrics.

ACKNOWLEDGEMENTS

The financial support from the Universities of Zhejiang Province (YB201506), the National Training Programs of Innovation and Entrepreneurship for Undergraduates (201710354004) and the Public Technology Application Programme (Analysis and Testing) of Zhejiang Province (2017C37034) is gratefully acknowledged. In addition, the financial support from the Constructing Programme of Zhejiang Province Experimental Teaching Demonstrating Center (84011002Z) is also acknowledged.

REFERENCES

- [1] Z. Shi, I. Wyman, G. Liu, H. Hu, H. Zou, J. Hu, *Polymer* 2013; 54: 6406-6414.
- [2] E. S. Abdel-Halim, F. A. Abdel-Mohdy, M. M. G. Fouda, S. M. El-Sawy, I. A. Hamdy, S. S. Al-Deyab, *Carbohydr Polym* 2011; 86: 1389-1394.
- [3] C. H. Xue, J. Chen, W. Yin, S. T. Jia, J. Z. Ma, *Appl Surf Sci* 2012; 25: 82468-2472.
- [4] M. Rehan, A. Hartwig, M. Ott, L. Gätjen, R. Wilken, *Surf Coat Tech* 2013; 219: 50-58.
- [5] J. Alongi, F. Carosio, A. Frache, G. Malucelli, *Carbohydr Polym* 2013; 92: 114-119.
- [6] Ş. S. Uğur, M. Sarıışık, A. H. Aktaş, *Mater Res Bull* 2011; 46: 1202-1206.
- [7] Y. Lu, Q. Liang, L. Xue, *Appl Surf Sci* 2012; 258: 4782-4787.
- [8] J. Molina, J. Fernández, A. I. Ríó, J. Bonastre, F. Cases, *Appl Surf Sci* 2013; 279 : 46-54.
- [9] D. Liu, W. Zhao, S. Liu, Q. Cen, Q. Xue, *Surf Coat Tech* 2016; 286: 354-364.
- [10] W. Zeng, L. Shu, Q. Li, S. Chen, F. Wang, X. M. Tao, *Adv Mater* 2014; 26: 5310- 5336.

- [11] X. Ji, Y. Xu, W. Zhang, L. Cui, J. Liu, Compos Part A 2016; 87: 29-45.
- [12] Q. Zhou, X. Ye, Z. Wan, C. Jia, J Power Sources 2015; 296: 186-196.
- [13] M. S. Khalilabad, M. E. Yazdanshenas, Carbohyd Polym 2013; 96 :190-195.
- [14] I. A. Sahito, K. C. Sun, A. A. Arbab, M. B. Qadir, S. H. Jeong, Electrochim Acta 2015; 173: 164-171.
- [15] K. Javed, C. M. A. Galib, F. Yang, C. M. Chen, C. Wang, Synthetic Met 2014; 193: 41-47.
- [16] M. Tian, X. Hu, L. Qu, S. Zhu, Y. Sun, G. Han, Carbon 2016; 96: 1166-1174.
- [17] X. Tang, M. Tian, L. Qu, S. Zhu, X. Guo, G. Han, K. Sun, X. Hu, Y. Wang, X. Xu, Synthetic Met 2015; 202: 82-88.
- [18] M. Tian, L. Qu, X. Zhang, K. Zhang, S. Zhu, X. Guo, G. Han, X. Tang, Y. Sun, Carbohyd Polym 2014; 111: 456-462.
- [19] W. S. Hummers, R. E. Offeman, J Am Chem Soc 1958; 80: 1339-1339.
- [20] M. Mathesh, J. Liu, N. D. Nam, S. K. H. Lam, R. Zheng, C. J. Barrow, W. Yang, J Mater Chem C 2013; 1: 3084-3090.
- [21] E. Y. Choi, T. H. Han, J. Hong, J. E. Kim, S. H. Lee, H. W. Kim, S. O. Kim, J Mater Chem 2010; 20: 1907-1912.
- [22] C. J. Jahagirdar, L. B. Tiwari, J Appl Polym Sci 2004; 94: 2014-2021.
- [23] R. Li, C. Chang, J. Zhou, L. Zhang, W. Gu, C. Li, S. Liu, S. Kuga, Ind Eng Chem Res 2010; 49: 11380-11384.
- [24] K. S. Novoselov, A. K. Geim, S. V. Morozov, D. Jiang, Y. Zhang, S. V. Dubonos, I. V. Grigorieva, A. A. Firsov, Science 2004; 306: 666-669.
- [25] N. D. Tissera, R. N. Wijesena, J. R. Perera, K. M. N. Silva, G. A. J. Amaratunge, Appl Surf Sci 2015; 324: 455-463.

AUTHORS' ADDRESSES

Wen Wu

Huanxia Zhang

Hui Ma

Jianda Cao

Guanglin Chen

Jiaying University

No. 56 North Yuexiu Road

Jiaying, Zhejiang 314001

CHINA